Molecular Crystals and Liquid Crystals

Publication details, including instructions for authors and subscription information:
http://www.informaworld.com/smpp/title~content=t713644168

LED-Lit LCD TVs

Ruibo Lu [a]; Sebastian Gauza [a]; Shin-Tson Wu [a]
[a] College of Optics and Photonics, University of Central Florida, Orlando, FL, USA

PLEASE SCROLL DOWN FOR ARTICLE

Taylor & Francis
Taylor & Francis Group

LED-Lit LCD TVs

Ruibo Lu, Sebastian Gauza, and Shin-Tson Wu

College of Optics and Photonics, University of Central Florida,
Orlando, FL, USA

Recent advances of LED-lit LCD TVs are reviewed. The influence of LED backlight on the color performance, electro-optic characteristics of the LCD TVs, and color-sequential LCDs are emphasized. The LED backlit LCDs not only exhibits a wider color gamut but also has a ~ 1.3–2.5X smaller color shift than that of CCFL-BLU especially when there are no color filters used. Wide view angle of higher than 100:1 within the 85° viewing cone can be guaranteed with the optimal film compensation schemes. The LED light source as a 2D adaptive dimming backlight not only enhances the viewing angle but also lowers the power consumption. A thin twisted-nematic cell filled with a high birefringence exhibits a response time less than 2 ms, which is attractive for color sequential display using RGB LEDs.

Keywords: backlight; light emitting diodes; liquid crystal display

1. INTRODUCTION

Light emitting diodes (LEDs)-lit liquid crystal displays (LCDs) are emerging rapidly because they offer tremendous advantages over the conventional cold-cathode fluorescent lamp (CCFL) in wider color gamut, smaller color shift, higher brightness, reduced motion artifacts without brightness and lifetime penalties, higher dimming contrast ratio, and reduced power consumption [1–3]. For high performance LCD TVs, wide viewing angle, high contrast ratio, fast response time without image blurring, good color saturation and small color shift are the major technical challenges. The adoption of LED as LCD backlight is a promising approach to overcome the above technical challenges for TV applications [4,5].

246

In this paper, we review the recent advances of LED-lit LCD TVs. We focus on discussing the influence of LED backlight on the color performance, electro-optic characteristics of the LCD TVs, and color-sequential LCDs. We compare the color gamut and color shift of the LCDs using RGB LEDs and CCFL as the backlight units through the quantitative simulation. An optimal compensation schemes is discussed to obtain wide view angle which reduces the light leakage from the crossed linear polarizers and the LC cell itself at off-axis angles. The LED light source can be used as a 2D adaptive dimming backlight, which can further enhance the viewing angle and lower the power consumption at the same time. A thin twisted-nematic (TN) cell with less than 2 ms response time is demonstrated for color sequential LCDs using RGB LEDs.

2. COLOR PERFORMANCE OF LED-LIT LCD

2.1. Color Gamut

Color performance is an important factor in evaluating the image quality of a display device. The color gamut of a display panel is referred to the range of colors that it can reproduce or distinguish. For an LCD device such as a computer monitor or a TV panel, the color gamut can be plotted with the device's RGB primaries. Figure 1 shows the transmission spectra of the CCFL and LED backlight units (BLUs) and color filters (CFs). The CCFL-BLU shown here is a commercial wide gamut one. The LED-BLU consists of a series of separate RGB LEDs, where the red LED (AlInGaP) has a peak wavelength at $R \sim 630$ nm and a full-width-half-maximum FWHM ~ 22 nm, the green LED (InGaN) has a peak wavelength at $G \sim 530$ nm and FWHM ~ 43 nm, and the blue LED (InGaN) has a peak wavelength at $B \sim 460$ nm and FWHM ~ 24 nm [1]. The CFs have the average peak wavelengths at $R \sim 650$ nm, $G \sim 550$ nm and $B \sim 450$ nm. It can be seen that the RGB peak wavelengths of LED-BLU match better with those of CFs, and its respective bandwidth is narrower and without side-lobes as compared to that of CCFL.

Figure 2 is a plot of the RGB primaries through the film-compensated MVA LCD panel using CCFL, LED with color filters, and RGB LED without color filters [6]. The color gamut defined by the RGB LED color points from LED-BLU with color filters in the color diagram is larger than that of the CCFL primaries and the National Television System Committee (NTSC) standard primaries. This means it is possible to obtain a greater than 100% NTSC color gamut by properly selecting the LED colors and color filters. As for the primaries of the
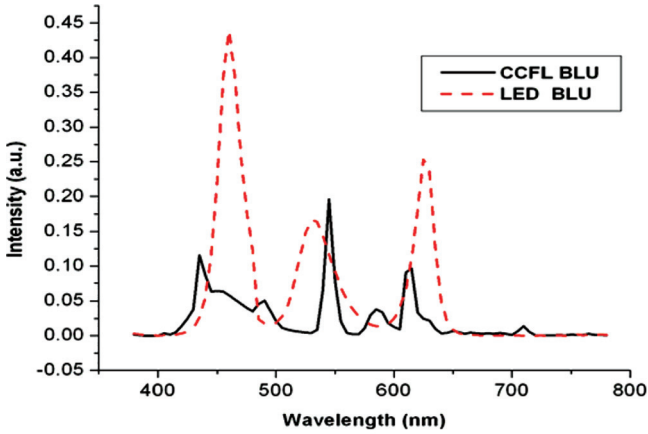
(a)
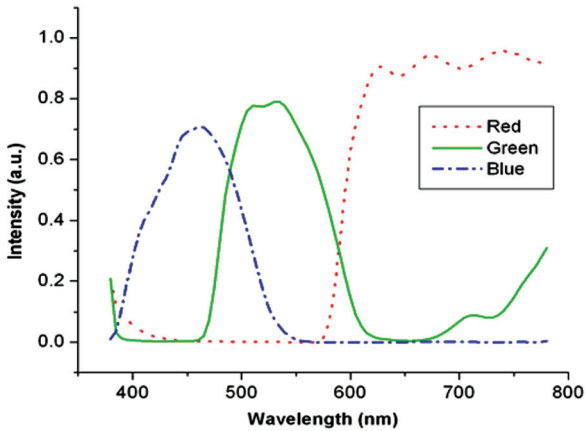
(b)

FIGURE 1 The emission spectra of (a) CCFL- & LED-BLU, and (b) the transmission spectra of CFs.

separate RGB LEDs without color filters, the color space can be further widened from 112.3% to 128.6%. The color gamut of an LCD device using the conventional CCFL-BLU is usually about 75% NTSC. Meanwhile, even though a wide gamut CCFL-BLU has been commonly adopted by LCD industry, the color gamut achieved by the CCFL backlight is 93.5% of the NTSC standard, which is still narrower than that of LED backlights. This is because the peak transmittance of the RGB primary colors of LED-BLU matches better with
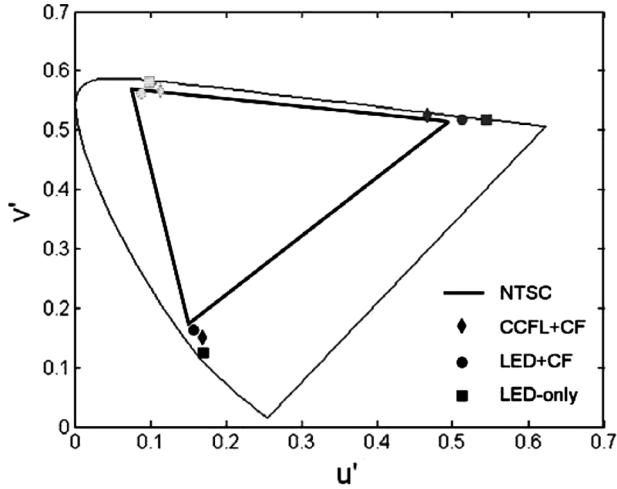
FIGURE 2 The RGB primaries through the MVA-LCD panel for different backlights and NTSC standard primaries on the CIE 1976 UCS diagram.

those of color filters and their respective narrower bandwidth. The color gamut can be further widened with multi-primary LEDs [7].

2.2. Color Shift

Color shift is a parameter determining the color uniformity of an LCD panel at different viewing directions. The CIE 1976 uniform chromaticity scale (UCS) diagram, which is also called (u', v') diagram, has been commonly used to present the equidistant chromaticity scales [8,9]. The (u', v') coordinates are related to the (x, y) coordinates in CIE 1931 by the following equations:

$$
\begin{aligned}
u' &= \frac{4X}{X + 15Y + 3Z} = \frac{4x}{-2x + 12y + 3} \\
v' &= \frac{9Y}{X + 15Y + 3Z} = \frac{9y}{-2x + 12y + 3}
\end{aligned}
\tag{1}
$$

Based on Eq. (1), $\Delta u'v'$ at any two positions (1 and 2) can be calculated using the following formula

$$
\Delta u'v' = \sqrt{(u'_2 - u'_1)^2 + (v'_2 - v'_1)^2}.
\tag{2}
$$

To characterize the color shift in an LCD TV, $[u'_2, v'_2]$ represent the $[u', v']$ values at an oblique viewing angle while $[u'_1, v'_1]$ are usually referred to the $[u', v']$ values at normal viewing angle. To calculate

the angular color uniformity under different backlights, we redefine Eq. (2) as

$$\Delta u'v' = \sqrt{(u'_{max} - u'_{min})^2 + (v'_{max} - v'_{min})^2}, \qquad (3)$$

where $[u'_{max}\ v'_{max}]$ and $[u'_{min}, v'_{min}]$ represent the maximum and minimum $[u', v']$ values at the full-bright state between the 0–80° viewing range.

For the angular color shift of the film-compensated MVA LCD under LED-BLU with CFs, we obtain $\Delta u'v' = (0.0110, 0.0274, 0.1115)$ at RGB primaries as shown in Table 1 [6]. To compare the angular color uniformity of the film-compensated MVA LCD with different backlights, we obtain $\Delta u'v' = (0.0159, 0.0343, 0.1271)$ for CCFL-BLU with CFs, and $\Delta u'v' = (0.0083, 0.0254, 0.0511)$ for RGB LED-BLU without CFs at the respective RGB primaries. The LED backlit MVA-LCD shows ~1.35X better angular color uniformity in green and ~2X in red and blue primaries than the CCFL-based MVA-LCD.

Figure 3 shows the simulated angular dependent $\Delta u'v'$ of MVA LCD backlit by different light sources as observed from the horizontal ($\phi = 0°$) viewing direction at the full-bright state. The RGB curves are more or less symmetric along $\theta = 0°$ and the $\Delta u'v'$ value increases as the theta angle increases. No matter which backlight is used, blue color always has the largest $\Delta u'v'$ value, followed by green and then red. However, human eyes are less sensitive to blue colors. In the region that $|\theta| > 0°$, the $\Delta u'v'$ of LED backlit MVA LCD with CFs is smaller than that of the CCFL-BLU with CFs for the respective RGB primaries. At $\theta = -80°$, $\Delta u'v' = (0.0099, 0.0235, 0.0981)$ for LED and $\Delta u'v' = (0.0139, 0.0292, 0.1090)$ for CCFL at the respective RGB primaries. From Figure 3, LED backlight is helpful for reducing color shift.

Also found in Figure 3, for each RGB primary the color shift of LED-only is much smaller than that of LED and CCFL with color filters. At $\theta = -80°$, the $\Delta u'v'$ values for the RGB primaries of the LED-only system are as low as $(0.0073, 0.0222, 0.0431)$, which is ~1.3–2.5X

TABLE 1 Color Shift of the Film-Compensated MVA LCD at Different Incident Angles

		CCFL + CF	LED + CF	LED-only
MVA	R	0.0159	0.0110	0.0083
	G	0.0343	0.0274	0.0254
	B	0.1258	0.1101	0.0511
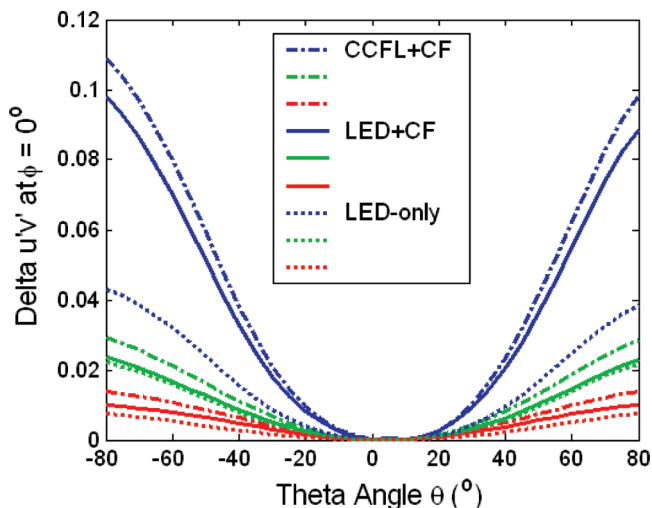
FIGURE 3 Color shift for RGB primaries under different backlights along the horizontal direction.

smaller than the conventional CCFL-BLU system. This advantage results from the narrower spectral bandwidth and less overlap of the RGB LED light sources. The color shift can be further reduced by improving the gamma curves at the oblique viewing angles. One of the effective methods is to employ dual-threshold approach in which a unit pixel is divided into two sub-pixels and each sub-pixel exhibits a different threshold voltage [10].

3. WIDE-VIEW LCDS

Lately, the viewing angle of film-compensated MVA and IPS LCDs has been dramatically improved. Hong et al [11] developed a computer simulation model based on the oblique-angle Jones matrix and Poincaré sphere to optimize the design of film-compensated MVA LCD. The absorption axes of polarizer and analyzer in the MVA LCD are in $0°$ and $90°$, respectively. Two A-plate films with equal thicknesses are laminated on the inner side of the crossed polarizers with their slow axes perpendicular to the absorption axes of the corresponding polarizers. Two equal-thickness C-plate films are placed between the A-plate films and the glass substrates. This phase compensation scheme is to reduce the light leakage from the crossed linear polarizers and the LC cell itself at off-axis angles.

Here, the entire LCD is treated as a multi-layer device with each layer approximated by a uniaxial anisotropic medium [12]. Assuming the interfacial reflections are negligible, the transmitted wave after the mth layer is related to the incident wave as

$$
\begin{bmatrix} E_\| \\ E_\perp \end{bmatrix}_m = J_m \cdot J_{m-1} \Lambda J_2 \cdot J_1 \cdot J_{ent} \cdot \begin{bmatrix} E_\| \\ E_\perp \end{bmatrix}_{in}, \tag{4}
$$

where J_m is the Jones matrix of the mth layer and J_{ent} is the correction matrix considering reflections on the air-polarizer interface.

The polarization state can be represented by Stokes parameters and plotted on Poincaré sphere as shown in Figure 4 [13]. The coordinates of Poincaré sphere are standard Stokes parameters S_1, S_2, and S_3. In Figure 4, A denotes the state of polarization absorbed by the analyzer, B denotes the state of polarization in front of the analyzer, D denotes the state of polarization emerging from the VA LC layer, G denotes the state of polarization emerging behind the first A-plate film, and P denotes the state of polarization passing through the polarizer.

To design the appropriate A-plate compensation films for minimizing the off-axis light leakage, first of all, we need to find $E_{\|\_G}$ and $E_{\perp\_G}$ (after the 1st A-plate film) in terms of the A-plate film thickness ($d_{A\text{-}plate}$) using Eq. (4), provided that the polarizer's thickness and refractive index and the A-plate's refractive index are known. Next,
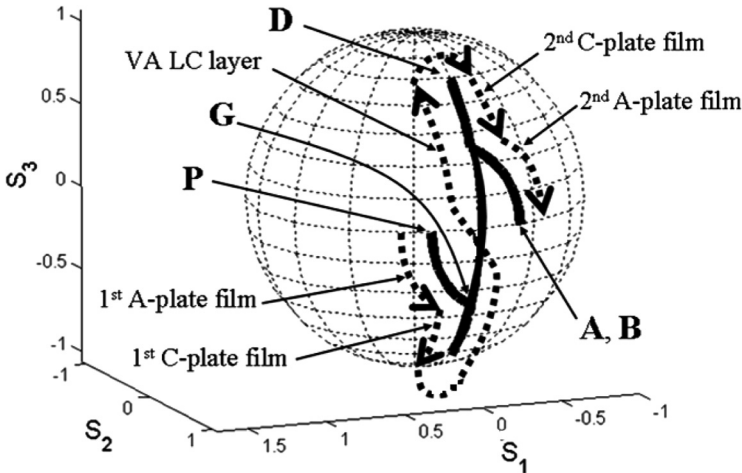

FIGURE 4 The states of polarization inside film-compensated MVA-LCD with optimal compensation films at $\theta = 70°$, $\phi = 45°$ and $\lambda = 550\,\text{nm}$ on the Poincaré sphere.

after S_1 of A and S_1 of P have been solved, we derive the following relationship

$$S_{1\_G} = \frac{(|E_{\|\_G}|^2 - |E_{\perp\_G}|^2)}{(|E_{\|\_G}|^2 + |E_{\perp\_G}|^2)} = \frac{(S_{1\_P} + S_{1\_A})}{2}. \tag{5}$$

Equation (5) can be further simplified as

$$H_1 \cdot \cos(K_1 \cdot d_{A-plate}) - L_1 = (S_{1\_P} + S_{1\_A})/2, \tag{6}$$

where constants H_1, K_1, and L_1 depend on the polarizer thickness, the refractive indices of the polarizer, and the A-plate film; and S_{1_A} represents S_1 of A and S_{1_P} is S_1 of P. Finally, $d_{A-plate}$ can be obtained in the following analytical form

$$d_{A-plate} = \frac{1}{K_1} \cdot \arccos\left(\frac{(S_{1\_P} + S_{1\_A})/2 + L_1}{H_1}\right). \tag{7}$$

To optimize the C-plate film, B should satisfy the conditions $S_{1\_B} = S_{1\_A}$ and $S_{3\_B} = S_{3\_A}$. Similarly, we first need to find $E_{\|\_B}$ and $E_{\perp\_B}$ (after the 2nd A-plate film) in terms of the C-plate thickness ($d_{C-plate}$). Next, applying $S_{1\_B} = S_{1\_A}$ yields

$$\frac{(|E_{\|\_B}|^2 - |E_{\perp\_B}|^2)}{(|E_{\|\_B}|^2 - |E_{\perp\_B}|^2)} = S_{1\_A}. \tag{8}$$

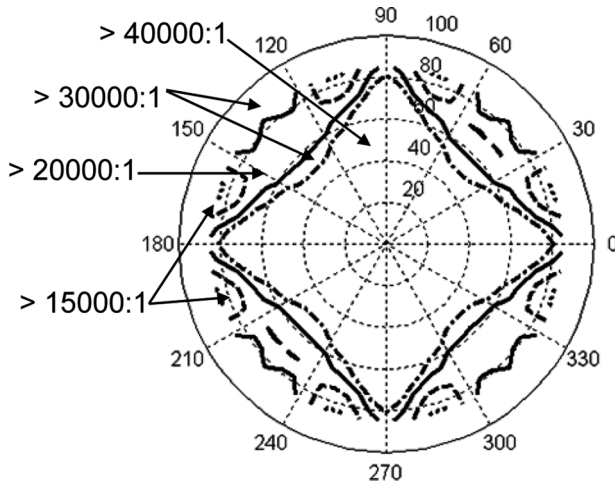**FIGURE 5** Isocontrast ratio of the four-domain VA LCD with compensation films optimized at $\theta = 70°$ and $\phi = 45°$.

After simplifying Eq. (8), the following expression can be derived

$$H_2 \cdot \cos(K_2 \cdot d_{C-plate}) + L_2 \cdot \sin(K_2 \cdot d_{C-plate}) = S_{1\_A}, \qquad (9)$$

where constants H_2, K_2, and L_2 depend on the thickness of the polarizer and the A-plate film, the LC cell gap, and the refractive indices of the polarizer, A-plate film, C-plate film, and LC material. Therefore, the thickness of each C-plate film $d_{C\text{-}plate}$ can be found from Eq. (9).

The above methodology is applied to design the MVA-LCD, where the compensation films are optimized at $\theta = 70°$, $\phi = 45°$, and $\lambda = 550$ nm. From Eq. (7), we find the A-plate thickness $d_{A-plate} = 26.62\,\mu$m and the d·Δn of each A-plate film is 93.17 nm. Using Eq. (9), we obtain the thickness of each C-plate film $d_{C-plate} = 21.54\,\mu$m. Therefore, the d·Δn of each C-plate film is -75.39 nm. With this optimal design, in the dark state, the polarization state in front of the analyzer equals to the polarization state absorbed by the analyzer at $\theta = 70°$ and $\phi = 45°$. Therefore, a theoretical contrast ratio higher than 10,000:1 over the

(a) Input image   (b) Backlight local dimming
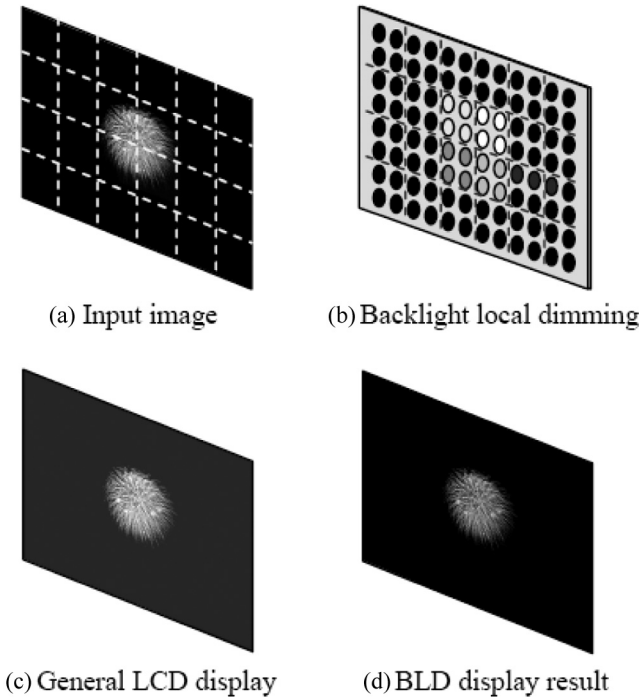
(c) General LCD display   (d) BLD display result

FIGURE 6 The working principle of backlight local dimming (BLD). (After Ref. 13)

$\pm 85°$ viewing cone is achieved, as plotted in Figure 5. Within $\pm 5\%$ manufacturing margin, the simulated contrast ratio maintains higher than 100:1 within the 85° viewing cone.

Since the contrast ratio is greatly influenced by the dark state, it is important to minimize the dark state in order to enhance the contrast ratio over a wide viewing range. The pixel compensated backlight dimming method has been proposed to improve the static contrast ratio for the LED-lit LCD [14]. The backlight luminance is dimmed locally along with the image contents, and pixel values are compensated synchronously according to the luminance profile of the dimmed backlight as shown in Figure 6. Static contrast ratio above 20,000:1 has been achieved on a large size LCD with the proposed method, and no obvious artifact effect was observed.

4. ADAPTIVE BACKLIGHT DIMMING

In the conventional LCD TVs, the backlight units are usually at the full luminance condition no matter bright or dark images are displayed. This leads to a relatively high power consumption and low contrast ratio due to light leakage in the dark state. The adaptive
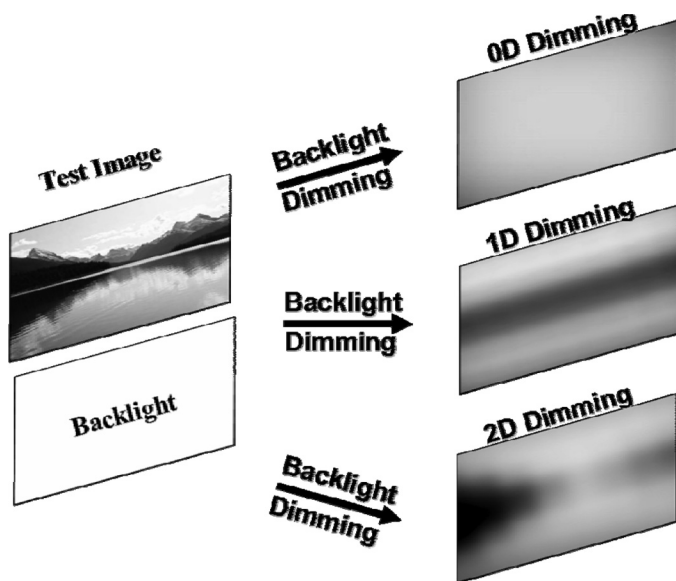

FIGURE 7 The different adaptive backlight dimming technologies. (After Ref. 14)

TABLE 2 The Comparison of Different LCD-TV Backlight Unites (BLUs)

Light source	Power range (%)			Control
	Minimum	Typical	Maximum	
CCFL	33	100	120	0D/1D
EEFL	20	100	120	0D/1D
HCFL	10	100	300	0D/1D
Low power RGB-LED	0	100	140	0D/1D/2D/2D color
Low power RGB-LED	0	100	200	0D/1D/2D/2D color
White LED	0	100	120	0D/1D/2D

backlight dimming approach has been proposed to enhance the image contrast and save the power consumption [7]. Figure 7 illustrates the different adaptive backlight dimming technologies [15]. The most common methods are 0D dimming or 1D scanning fluorescent lamps (FL) based on the image average picture level or the histogram. The LCD image data are adjusted to compensate the brightness correspondingly. RGB LEDs can be driven separately in two-dimensions, so LED light source can be used as a 2D adaptive dimming backlight.

A high contrast LCD-TV using 2D dynamic LED backlight has been proposed [16], where the whole backlight is divided into multiple regions. Each region's luminance and chroma is controlled independently. Since LED can be totally turned off, the image contrast can be enhanced significantly. With the adaptive dimming LED backlight, a high dynamic contrast ratio of 100,000:1 can be easily obtained [17]. In combination with the adaptive dimming and boosting backlight technologies, the temporal contrast ratio is basically infinity by adopting the 2D-dimming scheme. Meanwhile, as shown in Table 2, the average power consumption can be saved up to 50% in comparison with that using FL backlight [18].

5. COLOR SEQUENTIAL LED-LCD

Fast response time is critically important for minimizing the motion blur or realizing a color sequential display using RGB LEDs [19]. High birefringence (Δn) liquid crystals [20] are attractive for improving the response time of a display device through cell gap (d) reduction [21–22]. In a $90°$ twisted-nematic (TN) cell, the Gooch-Tarry first minimum leads to $d\Delta n/\lambda = \sqrt{3/2}$, where λ is the wavelength [23]. Meanwhile, the decay time is related to the cell gap and visco-elastic coefficient (γ_1/K_{22}) as: $\tau_{off} = \gamma_1 d^2/(K_{22}\pi^2)$. In the RGB LED-backlit color-sequential LCDs, the pigment color filters can be eliminated which not only
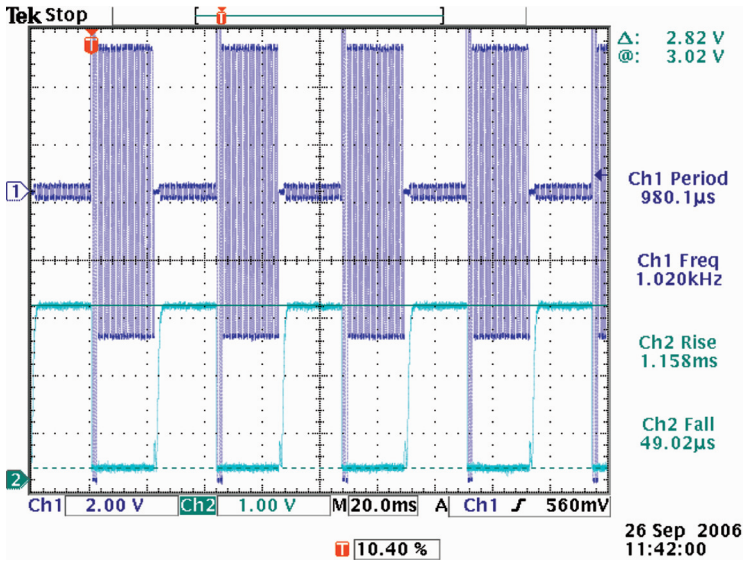
FIGURE 8 Electro-optical response of a 1.6-μm TN cell filled with a high birefringence nematic LC mixture at $\lambda = 633$ nm and T = 35°C.

reduces the LCD cost but also triples the device resolution and optical efficiency. However, to avoid color break up the LC response time (gray to gray) should be kept below 5 ms. Commercially available high Δn TFT-grade LC mixtures usually have Δn ~ 0.2. Under such a circumstance, to satisfy the Gooch-Tarry's first minimum condition would require a cell gap of ~ 2.5 μm. The resultant response time would still exceed 5 ms.

Our group has developed a high Δn (~ 0.35) and low viscosity LC mixture [24]. We filled the LC mixture into a TN cell with d ~ 1.6 μm and measured its rise and decay time. Figure 8 shows an example of the electro-optical response of the 1.6-μm TN cell. At $\lambda = 633$ nm and 35°C temperature, the obtained rise and decay time is 0.05 ms and 1.16 ms, respectively. Such a driving scheme includes overdrive technique with ON voltage of 5 V. Further increasing temperature reduces the response time to 0.03 ms and 0.96 ms.

Table 3 summarizes the measured data at the specified temperatures. The fast rise time results from the overdrive voltage [25–27], but the decay time is independent of the overdrive voltage. The decay time of the 1.6-μm TN cell at 25°C is 1.71 ms. As the temperature

TABLE 3 Measured Rise and Decay Times of the 1.6-μm TN LC Cell

Temperature (°C)	Rise Time (ms)	Decay Time (ms)	Total (ms)
25	0.07	1.71	1.78
35	0.04	1.14	1.18
45	0.03	0.94	0.97
50	0.03	0.69	0.72

increases, both rise time and decay time decrease. The sum of the rise and decay time is less than 2 ms.

CONCLUSION

The recent advances of LED-lit LCD TVs have been reviewed. The influence of LED backlight on the color performance, electro-optic characteristics of the LCD TVs, and color-sequential LCDs are discussed. We have obtained quantitative color performance results of the multi-domain MVA LCDs using RGB LEDs and CCFL as the backlight units. The LED backlit LCDs not only exhibits a wider color gamut but also has a ∼1.3–2.5X smaller color shift than that of CCFL-BLU especially when no color filters are used. Wide view angle can be guaranteed with the optimal compensation schemes which reduce the light leakage from the crossed linear polarizers and the LC cell itself at off-axis angles. The LED light source can be used as a 2D adaptive dimming backlight, which can further enhance the viewing angle and save the power consumption on the same time. A thin cell gap TN cell filled with a high birefringence is investigated for the color sequential display using RGB LEDs, which has a fast response time of less than 2 ms for both the rise and decay periods. In conclusion, LEDs as the backlight source of LCDs are very promising and wide spread applications of LED backlights for high-performance LCD TVs are foreseeable.

REFERENCES

[1] Harbers, G. & Hoelen, C. (2001). *SID Symposium Digest*, *32*, 702.
[2] Anandan, M. (2006). *SID Symposium Digest*, *37*, 1509.
[3] Shirai, T., Shimizukawa, S., Shiga, T., Mikoshiba, S., & Käläntär, K. (2006). *SID Symposium Digest*, *37*, 1520.
[4] Lu, R., Hong, Q., Ge, Z., & Wu, S. T. (2006). *Opt. Express*, *14*, 6243.

[5] Kakinuma, K., Shinoda, M., Arai, T., Shibata, H., Shirakuma, T., Kawase, M., Uba, T., Kumakura, T., Haga, S., & Matsumoto, T. (2007). *SID Symposium Digest*, *38*, 1232.

[6] Lu, R., Hong, Q., Wu, S. T., Peng, K. H., & Hsieh, H. S. (2006). *J. Display Technology*, *2*, 319.

[7] Roth, S., Weiss, N., Chorin, M. B., David, I. B., & Chen, C. H. (2007). *SID Symposium Digest*, *38*, 34.

[8] Wyszecki, G. & Stiles, W. (1982). *Color Science–Concepts and Methods, Quantitative Data and Formulate (2nd Edition)*, Wiley: New York.

[9] Hunt, R. (1991). *Measuring Colour (2nd Edition)*, West Sussex: Ellis Horwood.

[10] Lu, R., Wu, S. T., & Lee, S. H. (2008). *Appl. Phys. Lett.*, *92*, 051114.

[11] Hong, Q., Wu, T. X., Zhu, X., Lu, R., & Wu, S. T. (2005). *Appl. Phys. Lett.*, *86*, 121107.

[12] Lien, A. (1990). *App. Phys. Lett.*, *57*, 2767.

[13] Huard, S. (1997). *Polarization of Light*, Wiley: New York.

[14] Chen, H., Sung, J., Ha., & Park, Y. (2007). *SID Symposium Digest*, *38*, 1339.

[15] Huang, Y. P., Lin, F. C., Liao, C. Y., Hsu, Y. T., Liao, L. Y., Chen, C. H., Shieh, H. P., Huang, W. K., Tsao, C. H., Hung, J. M., & Yeh, S. C. (2007). *Proc. Asia Opt. Fiber Comm. & Optoelectronics Expo. and Conf.*, 100.

[16] Shiga, T. & Mikoshiba, S. (2003). *SID Symposium Digest*, *34*, 1364.

[17] Peng, H. J., Zhang, W., Hung, C.-K., Tsai, C.-J., Ng, K.-W., Chen, S., Huang, D., Chueng, Y.-L., & Liu, Y. (2007). *SID Symposium Digest*, *38*, 1336.

[18] de Greef, P. & Hulze, H. G. (2007). *SID Symposium Digest*, *38*, 1332.

[19] Lee, J. H., Zhu, X., & Wu, S. T. (2007). *J. Display Technology*, *3*, 2.

[20] Gauza, S., Wang, H., Wen, C. H., Wu, S. T., Seed, A., & Dabrowski, R. (2003). *Jpn. J. Appl. Phys.*, *42*, 3463.

[21] Wu, S. T. & Efron, U. (1986). *Appl. Phys. Lett.*, *48*, 624.

[22] Jiao, M., Ge, Z., Song, Q., & Wu, S. T. (2008). *Appl. Phys. Lett.*, *92*, 061102.

[23] Gooch, C. H. & Tarry, H. A. (1975). *J. Phys. D.*, *8*, 1575.

[24] Gauza, S., Zhu, X., Wu, S. T., Piecek, W., & Dabrowski, R. (2007). *J. Display Technology*, *3*, 250.

[25] Wu, S. T. & Wu, C. S. (1988). *Appl. Phys. Lett.*, *53*, 1794.

[26] Wu, S. T. & Wu, C. S. (1989). *J. Appl. Phys.*, *65*, 527.

[27] Liang, X., Lu, Y. Q., Wu, Y. H., Du, F., Wang, H. Y., & Wu, S. T. (2005). *Jpn. J. Appl. Phys.*, *44*, 1292.